

On the Configuration Resulting from Oxidative Addition of RX to Pd(PPh₃)₄ and the Mechanism of the *cis*-to-*trans* Isomerization of [PdRX(PPh₃)₂] Complexes (R = Aryl, X = Halide)[†]

Arturo L. Casado and Pablo Espinet*

Departamento de Química Inorgánica, Facultad de Ciencias, Universidad de Valladolid, E-47005 Valladolid, Spain

Received October 31, 1997

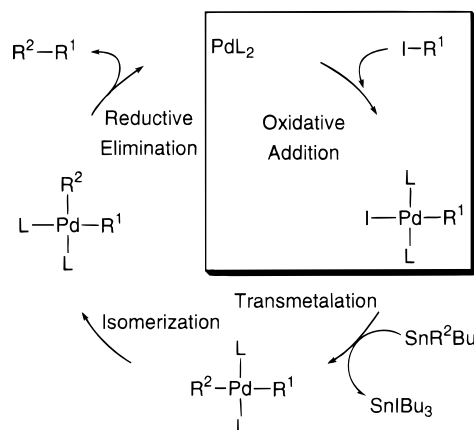
The oxidative addition of RI to Pd(0) and further *cis*-to-*trans* isomerization, which are involved in the Stille reaction and other Pd-catalyzed syntheses, have been studied. C₆Cl₂F₃I (**1**, C₆Cl₂F₃ = 3,5-dichlorotrifluorophenyl) adds to Pd(PPh₃)₄ in THF at room temperature giving *cis*-[Pd(C₆Cl₂F₃)I(PPh₃)₂] (**2**), which could be isolated before isomerization to the more stable *trans*-[Pd(C₆Cl₂F₃)I(PPh₃)₂] (**3**). A ¹⁹F NMR kinetic study of the isomerization of **2** in THF at 322.6 K reveals a first-order law $r_{\text{iso}} = k_{\text{iso}}[\mathbf{2}]$, with $k_{\text{iso}} = f + g[\mathbf{2}]_0 + (h + i[\mathbf{2}]_0)/([\text{PPh}_3] + j)$ ($f = (1.66 \pm 0.03) \times 10^{-4} \text{ s}^{-1}$, $g = (2.5 \pm 0.2) \times 10^{-3} \text{ mol}^{-1} \text{ L s}^{-1}$, $h = (1.3 \pm 0.7) \times 10^{-8} \text{ mol L}^{-1} \text{ s}^{-1}$, $i = (4 \pm 2) \times 10^{-7} \text{ s}^{-1}$, and $j = (1.4 \pm 0.7) \times 10^{-5} \text{ mol L}^{-1}$). A four-pathway mechanism accounts for these results: Two are assigned to the associative replacements of PPh₃ coordinated to **2** by an iodide ligand of I–[Pd] (I–[Pd] = **2** or **3**), both THF-assisted (coefficient h) or direct (coefficient i), leading to a monoiodide-bridged intermediate *cis*-{Pd(C₆Cl₂F₃)I(PPh₃)(μ-I)-[Pd]}. The later rearranges via terminal-for-bridging iodide exchange to *trans*-{Pd(C₆Cl₂F₃)I(PPh₃)(μ-I)-[Pd]}, which is finally cleaved by PPh₃ yielding complex **3**. The other two concurrent pathways are assigned to the isomerization via two consecutive Berry pseudorotations in the pentacoordinated species derived from **2** by coordination of THF (coefficient f) or I–[Pd] (coefficient g). The apparent activation entropy associated with k_{iso} is negative ($\Delta S^\ddagger = -21 \pm 3 \text{ J K}^{-1} \text{ mol}^{-1}$), in agreement with the proposed bimolecular mechanisms.

Introduction

The oxidative addition of aryl halides or pseudohalides (RX) to zerovalent Pd complexes is the first step in many catalyzed cross-coupling reactions, such as the Stille reaction (Scheme 1) and related processes.¹ The isolated or postulated products of the oxidative addition are commonly *trans*-[PdRXL₂] (L = neutral ligand). Nevertheless, the mechanism of the oxidative addition has been established to proceed usually via a concerted insertion of highly reactive coordinatively unsaturated species PdL₂ or Pd(L-L) (L-L = diphosphine) into the RX σ bond.² Consequently, even for monodentate ligands, a *cis*-[PdRXL₂] complex must be formed first, although it further isomerizes to the *trans* isomer.

To the best of our knowledge, a *cis* isomer (R = substituted uracil, L = PPh₃) has been isolated from an oxidative addition in only one case.³ Its isomerization to the *trans* isomer was retarded by addition of neutral

Scheme 1



ligand L, and a dissociative mechanism, proceeding via a three-coordinate intermediate,^{4,5} was postulated (Scheme 2).

In the course of our studies on the mechanism of the Stille couplings, using perhaloaryl iodides to facilitate

[†] Dedicated to Prof. P. Royo on occasion of his 60th birthday.

(1) (a) Farina, V.; Roth, G. P. in *Advances in Metal-Organic Chemistry*; Liebeskind, L. S., Ed.; JAI Press: Greenwich, CT, 1996, Vol. 5, pp 1–53. (b) Farina, V. In *Comprehensive Organometallic Chemistry II*; Abel, E. W., Stone, F. G. A., Wilkinson, G., Eds.; Pergamon: Oxford, 1995, Vol. 12, Chapter 3.4. (c) Brown, J. M.; Cooley, N. A. *Chem. Rev.* **1988**, *88*, 1131–1146.

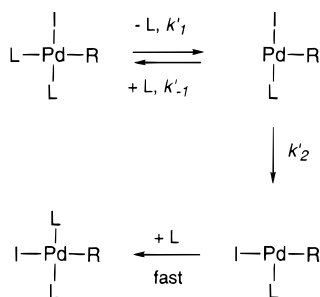
(2) (a) Amatore, C.; Broeker, G.; Jutand, A.; Khalil, F. *J. Am. Chem. Soc.* **1997**, *119*, 5176–5185. (b) Amatore, C.; Jutand, A.; Suarez, A. *J. Am. Chem. Soc.* **1993**, *115*, 9531–9541. (c) Amatore, C.; Pflüger, F. *Organometallics* **1990**, *9*, 2276–2282.

(3) Urata, H.; Tanaka, M.; Fuchikami, T. *Chem. Lett.* **1987**, 751–754.

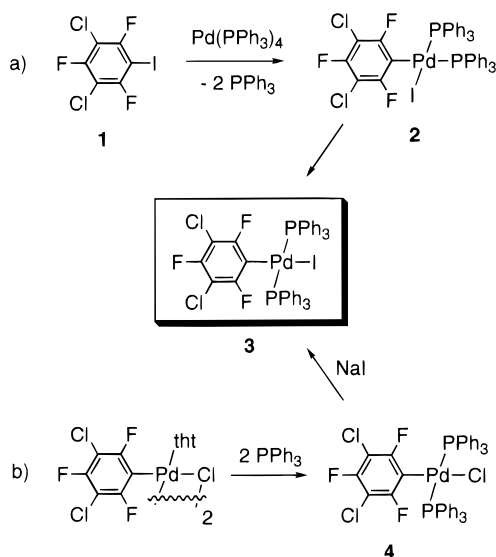
(4) Minniti, D. *Inorg. Chem.* **1994**, *33*, 2631–2634.

(5) (a) Tatsumi, K.; Hoffmann, R.; Yamamoto, A.; Stille, J. K. *Bull. Chem. Soc. Jpn.* **1981**, *54*, 1857–1867. (b) Ozawa, F.; Ito, T.; Nakamura, Y.; Yamamoto, A. *Bull. Chem. Soc. Jpn.* **1981**, *54*, 1868–1880. (c) Komiya, S.; Albright, T. A.; Hoffmann, R.; Kochi, J. K. *J. Am. Chem. Soc.* **1976**, *98*, 7255–7265.

Scheme 2



Scheme 3



the isolation or detection of intermediates, we have found that the reaction of $C_6Cl_2F_3I$ ($C_6Cl_2F_3 = 3,5$ -dichlorotrifluorophenyl) with $Pd(PPh_3)_4$ (a very common catalyst precursor) produces cis - $[Pd(C_6Cl_2F_3)I(PPh_3)_2]$ (**2**), which slowly isomerizes to $trans$ - $[Pd(C_6Cl_2F_3)I(PPh_3)_2]$ (**3**) (the actual transmetalation catalyst in Scheme 1). Our kinetic studies on the isomerization step demonstrate the occurrence of four concurrent associative pathways.

Results and Discussion

The oxidative addition of $C_6Cl_2F_3I$ (**1**) to $Pd(PPh_3)_4$ yielded, after 5 h in toluene at $60^\circ C$, a 1:2 mixture of cis - $[Pd(C_6Cl_2F_3)I(PPh_3)_2]$ (**2**) and $trans$ - $[Pd(C_6Cl_2F_3)I(PPh_3)_2]$ (**3**). When the reaction was carried out in THF at room temperature for 1 h, only complex **2** was formed in quantitative yield. Upon heating, the $trans$ isomer **3** was then formed from **2** (Scheme 3, a). A sample of **3**, prepared in a different way (Scheme 3, b), could not be isomerized to **2**, proving that **3** is the thermodynamically more stable isomer. These results suggest that under catalytic conditions (usually $50^\circ C$, 20:1 ratio organic iodide:Pd) the first product formed is **2**, which then isomerizes to **3**.

The cis or $trans$ configurations of **2** and **3** were established by multinuclear NMR spectroscopy: The $^{31}P\{^1H\}$ NMR spectrum of **2** in $CDCl_3$ shows two resonances at 29.6 and 16.7 ppm, whereas the ^{19}F NMR spectrum shows a doublet of doublets at -90.63 ppm corresponding to the F_{ortho} atoms coupled with two inequivalent P atoms. On the other hand, the $^{31}P\{^1H\}$

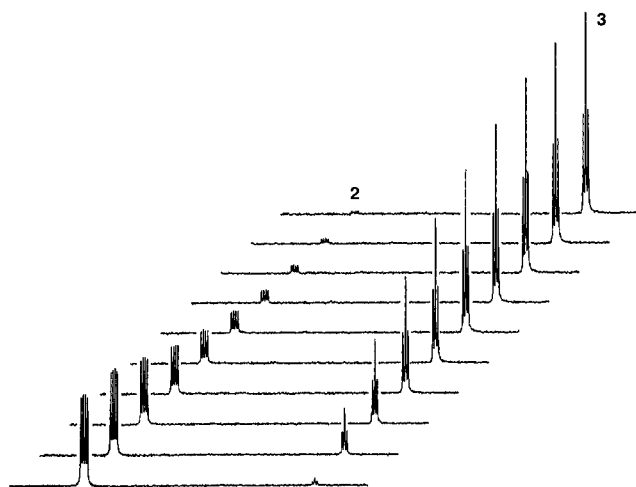


Figure 1. ^{19}F NMR (282 MHz, -85.0 to -88.5 ppm region) spectral sequence (10 min intervals) of the isomerization of cis - $[Pd(C_6Cl_2F_3)I(PPh_3)_2]$ (**2**, 10^{-2} mol L^{-1}) to $trans$ - $[Pd(C_6Cl_2F_3)I(PPh_3)_2]$ (**3**) at 315.7 K in THF.

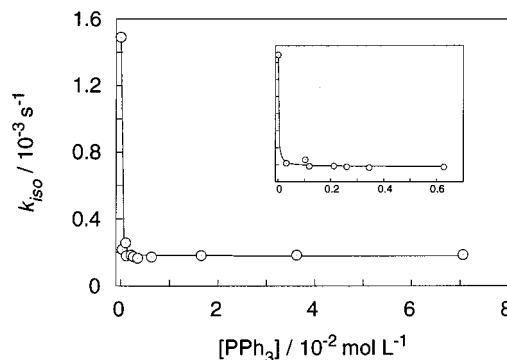


Figure 2. Retardation effect by addition of PPh_3 on the isomerization rate of cis - $[Pd(C_6Cl_2F_3)I(PPh_3)_2]$ (**2**, 10^{-2} mol L^{-1}) in THF at 322.6 K.

NMR spectrum of **3** shows only one resonance at 22.6 ppm, and its ^{19}F NMR spectrum exhibits a triplet at -92.48 ppm corresponding to the F_{ortho} atoms coupled with two equivalent P nuclei (the coupling constants are given in the Experimental Section).

The kinetics of the isomerization of **2** in THF and in chlorobenzene were studied by ^{19}F NMR spectroscopy (Figure 1) under a strictly oxygen-free N_2 atmosphere (see cautionary note in the Experimental Section). The reactions followed first-order rate laws $\ln([2]/[2]_0) = k_{iso}t$. The values of k_{iso} measured under different experimental conditions are given in Table 1.⁶

The results in Table 1 show that at a given temperature k_{iso} varies with $[PPh_3]$ and with the initial concentration of complex **2** ($[2]_0$). These experimental data have been analyzed by means of suitable representations in order to establish the rate law for the process.

The rate dependence on the concentration of added PPh_3 is shown in Figure 2. The isomerization of **2** in THF is at first sharply retarded by small amounts of free PPh_3 , but at $[PPh_3] > 10^{-2}$ mol L^{-1} the isomerization rate constant reaches a nearly constant k_{iso} value.

(6) (a) Wilkins, R. G. *Kinetics and Mechanism of Reactions of Transition Metal Complexes*, 2nd ed.; VCH: Weinheim, 1991. (b) Espenson, J. H. *Chemical Kinetics and Reaction Mechanisms*, 2nd ed.; McGraw-Hill: Singapore, 1995.

Table 1. First-Order Rate Constants k_{iso} for the Isomerization of *cis*-[Pd(C₆Cl₂F₃)I(PPh₃)₂] (**2**) to *trans*-[Pd(C₆Cl₂F₃)I(PPh₃)₂] (**3**)

solvent	<i>T</i> /K	[2] ₀ /10 ⁻³ mol L ⁻¹	[PPh ₃]/10 ⁻³ mol L ⁻¹	$k_{\text{iso}}/10^{-5}$ s ⁻¹
THF	296.2 ± 0.2	10.0 ± 0.2	0	6.5 ± 0.2
THF	300.9	10.0	0	11.4 ± 0.4
THF	304.9	10.0	0	20.0 ± 0.7
THF	310.4	10.0	0	39.2 ± 1.5
THF	315.7	10.0	0	72 ± 5
THF	322.6	4.72 ± 0.04	0	117 ± 4
THF	322.6	4.72	36.3 ± 0.5	17.7 ± 0.17
THF	322.6	10.0	0	149 ± 9
THF	322.6	10.0	0.320 ± 0.002	21.9 ± 0.2
THF	322.6	10.0	1.024 ± 0.006	25.8 ± 0.2
THF	322.6	10.0	1.190 ± 0.006	18.0 ± 0.2
THF	322.6	10.0	2.112 ± 0.006	18.4 ± 0.2
THF	322.6	10.0	2.602 ± 0.006	17.5 ± 0.2
THF	322.6	10.0	3.448 ± 0.006	16.7 ± 0.3
THF	322.6	10.0	6.272 ± 0.006	17.2 ± 0.2
THF	322.6	10.0	16.48 ± 0.06	18.2 ± 0.2
THF	322.6	10.0	36.3	18.5 ± 0.2
THF	322.6	10.0	70.6 ± 0.6	18.7 ± 0.2
THF	322.6	15.0 ± 0.2	0	153 ± 6
THF	322.6	15.0	36.3	20.7 ± 0.2
THF	322.6	20.0 ± 0.2	0	175 ± 7
THF	322.6	20.0	36.3	21.7 ± 0.2
THF	322.6	25.1 ± 0.3	0	186 ± 6
THF	322.6	25.1	36.3	22.5 ± 0.2
THF	326.1	10.0	0	208 ± 0.2
PhCl	322.6	4.01 ± 0.03	0	11.8 ± 0.2
PhCl	322.6	10.0	0	12.4 ± 0.2
PhCl	322.6	10.0	36.3	3.05 ± 0.07
PhCl	322.6	15.0	0	12.6 ± 0.2
PhCl	322.6	20.0	0	13.0 ± 0.2
PhCl	322.6	25.1	0	13.5 ± 0.2

Similar behavior was observed with chlorobenzene as the solvent. The nonlinear least-squares fitting of the data in Figure 2 gives eq 1,⁷ where $a = (1.81 \pm 0.10) \times$

$$k_{\text{iso}} = a + \frac{b}{[\text{PPh}_3] + c} \quad (1)$$

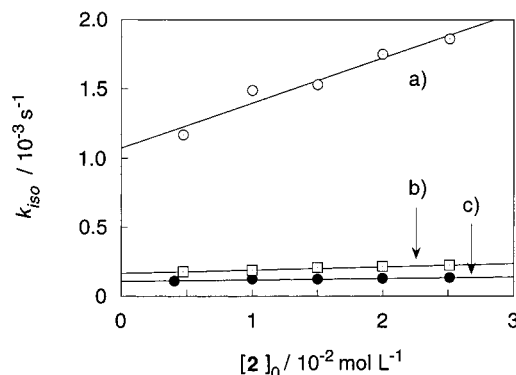
10^{-4} s⁻¹, $b = (1.7 \pm 0.9) \times 10^{-8}$ mol L⁻¹ s⁻¹, and $c = (1.3 \pm 0.7) \times 10^{-5}$ mol L⁻¹. This equation reveals two contributions to the isomerization rate. The first term, a , is independent of [PPh₃]. The second term is inversely dependent on [PPh₃] and corresponds to a pathway starting with PPh₃ dissociation from **2**. The later is responsible for the dramatic retarding effect of the added phosphine, which led to the suggestion of a dissociative mechanism in the literature.³

The dependence of the isomerization rate constant on the initial concentration of the starting complex **2** ([**2**]₀) is shown in Figure 3. Both in the absence (Figure 3a) and in the presence of an excess of PPh₃ (Figure 3b), k_{iso} varies following the two terms in eq 2, whose coefficients in each case are given in Table 2.

$$k_{\text{iso}} = d + e[\mathbf{2}]_0 \quad (2)$$

Equation 2 reveals two parallel contributions to the isomerization rate, one independent of the total concentration of the complexes (intercept d) and one proportional to [**2**]₀, suggesting an autocatalytic path-

(7) The study of the retarding effect of PPh₃ is extremely difficult because of the very sharp effect observed. For this reason, some coefficients in eq 3 have an appreciable imprecision. This difficulty has been noticed before in other kinetic work involving PPh₃; see, for example, ref 1a.

**Figure 3.** Dependence of the isomerization rate of *cis*-[Pd(C₆Cl₂F₃)I(PPh₃)₂] (**2**) with the initial concentration [**2**]₀ at 322.6 K: (a) in THF; (b) in THF with excess (3.63×10^{-2} mol L⁻¹) of PPh₃; (c) in PhCl.**Table 2.** Coefficients d and e for Eq 2 at 322.6 K

conditions	$d/10^{-4}$ s ⁻¹	$e/10^{-3}$ mol ⁻¹ L s ⁻¹
THF	10.8 ± 0.7	32 ± 4
THF with excess of PPh ₃ ^a	1.66 ± 0.03	2.5 ± 0.2
Chlorobenzene	1.09 ± 0.03	1.1 ± 0.2

^a (3.63 ± 0.05) $\times 10^{-2}$ mol L⁻¹.

way (slope e). The term which is independent of [**2**]₀ is clearly more important for THF than for chlorobenzene by about 1 order of magnitude. THF and chlorobenzene have a similar polarity, but the former coordinates more effectively to Pd(II) than the later.^{8,9} Hence, this observation suggests that the first term corresponds to a solvent-assisted pathway.

According to eq 2, each term in eq 1 must consist of two contributions, one constant and one proportional to [**2**]₀. After suitable numerical analysis, the four-term rate law given in eq 3 is obtained, where $f = (1.66 \pm 0.03) \times 10^{-4}$ s⁻¹, $g = (2.5 \pm 0.2) \times 10^{-3}$ mol⁻¹ L s⁻¹, $h = (1.3 \pm 0.7) \times 10^{-8}$ mol L⁻¹ s⁻¹, $i = (4 \pm 2) \times 10^{-7}$ s⁻¹, and $j = (1.4 \pm 0.7) \times 10^{-5}$ mol L⁻¹. The coefficients

$$k_{\text{iso}} = f + g[\mathbf{2}]_0 + \frac{h + i[\mathbf{2}]_0}{[\text{PPh}_3] + j} \quad (3)$$

given hold for THF at 322.6 K.

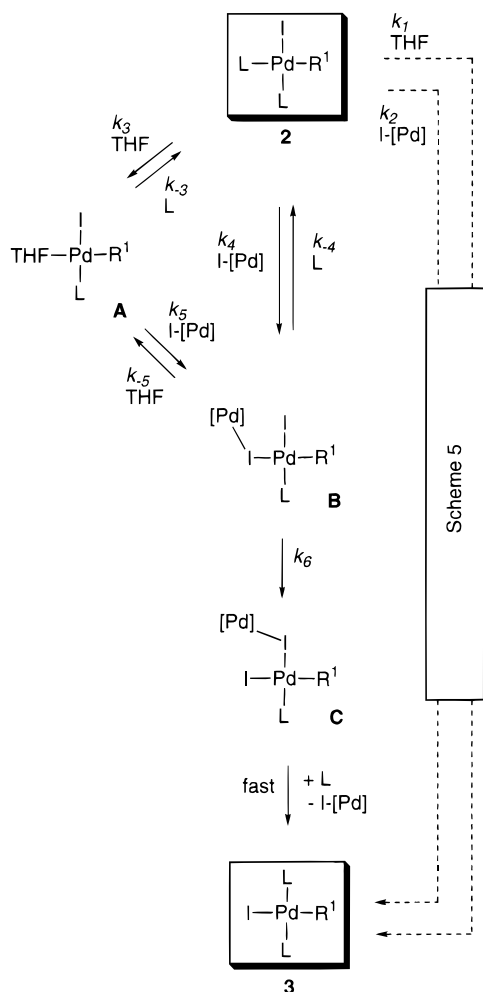
For each kinetic experiment, [PPh₃] and [**2**]₀ in eq 3 remain constant, rendering k_{iso} also constant and giving first-order dependence on [**2**].¹⁰ A simple dissociative pathway (Scheme 2) would also give first-order kinetics, but in such a case the rate constant k_{iso} should be independent of the initial concentration of reagent, [**2**]₀.^{6,11} Consequently, it must be discarded. The complexity of eq 3 reveals a more complicated situation involving at least four parallel pathways. The isomerization mechanism outlined in Scheme 4 accounts for this complexity.

(8) Catalán, J.; López, V.; Pérez, P.; Martín-Villamil, R.; Rodríguez, J.-G. *Liebigs Ann. Chem.* **1995**, 241–252.

(9) Complexes with THF coordinated to Pd(II) have been reported, see: Usón, R.; Fornies, J. *Adv. Organomet. Chem.* **1988**, 28, 219–297.

(10) In other words, although the isomerization is a second-order reaction (bimolecular), it shows (pseudo)first-order kinetics $\ln([\mathbf{2}]/[\mathbf{2}]_0) = k_{\text{iso}}t$ (see ref 6b, pp 16).

(11) The rate equation derived by applying the steady-state assumption to the dissociative Scheme 2 can be developed as in ref 4, giving an expression for the first-order rate constant $r_{\text{iso}} = k_{\text{iso}}[\mathbf{2}]$, where $k_{\text{iso}} = (k_1'k_2)/(k_{-1}'[\text{PPh}_3] + k_2)$. The first-order rate constant k_{iso} is independent of the initial concentration of the reagent [**2**]₀.

Scheme 4^a

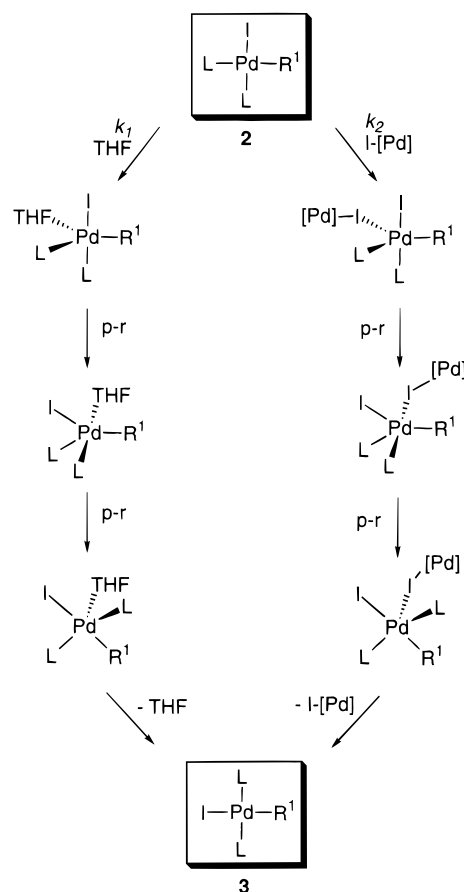
^a I-[Pd] stands for either **2** or **3**; $R^1 = C_6Cl_2F_3$; $L = PPh_3$.

There are two PPh_3 -insensitive (k_1 and k_2) and two PPh_3 -sensitive (k_3 and k_4) pathways. The corresponding theoretical rate expression (eq 4) is obtained by applying the steady-state approximation (see Appendix), under the simplification that complexes **2** and **3** catalyze the isomerization of **2** (autocatalytic pathways) with similar efficiency.¹²

$$r_{iso} = k_{iso}[2] = \left\{ k_1 + k_2[2]_0 + \frac{k_3k_6 + k_4k_6[2]_0}{k_{-4}[PPh_3] + k_6} \right\} [2] \quad (4)$$

The theoretical rate expression (eq 4) is consistent with our kinetic results. Comparing with the experimental rate law (eq 3), the following values for the elemental constants are obtained: $k_1 = (1.66 \pm 0.03) \times 10^{-4} \text{ s}^{-1}$, $k_2 = (2.5 \pm 0.2) \times 10^{-3} \text{ mol}^{-1} \text{ L s}^{-1}$, $k_3 = (9 \pm 5) \times 10^{-4} \text{ s}^{-1}$, $k_4 = (2.9 \pm 1.4) \times 10^{-2} \text{ mol}^{-1} \text{ L s}^{-1}$, $k_6/k_{-4} = (1.4 \pm 0.7) \times 10^{-5} \text{ mol L}^{-1}$.

The PPh_3 -sensitive pathways (Scheme 4, via k_3 and k_4) are the most important in THF. For $[2]_0 = 10^{-2} \text{ mol L}^{-1}$ and $[PPh_3] = 0$ at 322.6 K, reaction via k_3 accounts for 67% of the observed isomerization rate and reaction via k_4 for 21%. These pathways correspond to an associative substitution of PPh_3 from complex *cis*- $[PdR^1IL_2]$ (**2**) by an iodide ligand coordinated to either **2** or **3** (both represented by I-[Pd] in Scheme 4) to give a mono-bridged dimer **B**. The ligand substitution can

Scheme 5^a

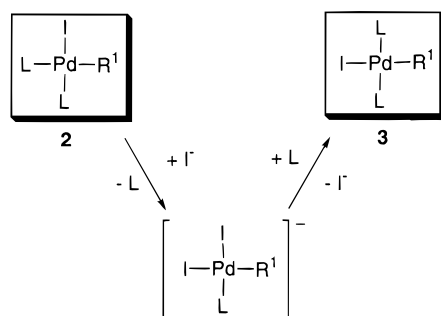
^a I-[Pd] stands for either **2** or **3**; $R^1 = C_6Cl_2F_3$; $L = PPh_3$; p-r = pseudorotation.

be THF-assisted (step k_3 , intermediate **A** is considered) or direct (step k_4); this two-term rate law is well-known in many substitution processes involving d^8 square-planar complexes.¹³ The intermediate **B** rearranges further (step k_6) by terminal-for-bridging iodide exchange to give **C**, which is finally cleaved by PPh_3 to yield complex **3**. The retarding effect of added free PPh_3 is due to the capture of intermediate **B**.

The two PPh_3 -insensitive pathways, via k_1 and k_2 , are less important in THF. For $[2]_0 = 10^{-2} \text{ mol L}^{-1}$ and $[PPh_3] = 0$ at 322.6 K, reaction via k_1 accounts for 12% of the observed isomerization rate whereas reaction via k_2 accounts for 2%. Since both pathways are unaffected by the addition of free PPh_3 , the mechanism should not involve the release of the neutral ligand. Plausible solvent-assisted and direct pathways are given in Scheme 5. The coordination of THF or I-[Pd] to complex **2** gives a pentacoordinated species, which can evolve through two consecutive Berry pseudorotations. Note that the release of PPh_3 from such pentacoordinated intermediates leads, respectively, to the intermediates **A** and **B** considered in Scheme 4; therefore, the

(12) If the isomerization was catalyzed only by **2**, a second-order rate law would be expected, $r_{iso} = k[2]^2$, giving a second-order dependence in time, $1/[2] = 1/[2]_0 + kt$. On the other hand, if the isomerization was catalyzed only by **3**, an autocatalytic law should hold, $r_{iso} = k([2]_0 - [2])[2]$, giving an S-shaped dependence in time, $\ln([2]_0/[2] - [2]) = kt$. Neither of these simple models explains the first-order kinetics, whereas eq 4 does.

(13) This two-terms rate law is common for substitution processes in planar complexes, see, for example: Belluco, U.; Cattalini, L.; Basolo, F.; Pearson, R. G.; Turco, A. *J. Am. Chem. Soc.* **1965**, *87*, 241–246.

Scheme 6^a^a R¹ = C₆Cl₂F₃; L = PPh₃.

two PPh₃-insensitive and the two PPh₃-sensitive mechanisms are connected.¹⁴

In chlorobenzene, a much less coordinating solvent, the isomerization rate is much lower and the contribution independent of [2]₀ is also very small. In this solvent, the contribution of a dissociative mechanism via a three-coordinate intermediate (as shown in Scheme 2), rather than a solvent-assisted pathway, could also be responsible for the constant contribution to *k*_{iso} (intercept in Figure 3c). In fact, with our data we cannot completely discount the occurrence of dissociative paths as an additional general contribution to the topomerization mechanism, even in THF. However, the lifetime of a three-coordinate intermediate in THF should be very short, as the coordinating solvent present in a large excess would quickly transform it into the THF-complex **A**, and consequently, its contribution should be unimportant. Moreover, it is known that the topomerizations of three-coordinate species are not fast in the case of palladium.^{5a}

The associative mechanisms proposed here are further supported by some other experimental facts. When the isomerization of **2** was carried out in THF saturated with NaI (scarcely soluble), complex **3** was formed very quickly, revealing a remarkable catalytic effect of the iodide ion. The rate of this disfavors a mechanism based on iodide dissociation from complex **2**, similar to that previously proposed for haloorganoplatinum(II) complexes,¹⁵ and supports the double-associative ligand substitution outlined in Scheme 6 and, indirectly, the autocatalyzed mechanism considered in Scheme 4. The iodide ligand, either free or complexed as I-[Pd], is playing a similar role in both schemes, but the lower nucleophilicity of I-[Pd] compared to that of the free iodide should produce a lower isomerization rate, as observed.

On the other hand, *apparent* activation parameters can be derived from an Eyring plot of ln(*k*_{iso}/T) vs 1/T. Since *k*_{iso} does not correspond to an elemental step but to a composite rate constant, it is strictly improper to apply transition-state theory. For this reason, we use the expression *apparent* Δ*H*[‡]_{iso} and Δ*S*[‡]_{iso} values. For [PPh₃] = 0, these are Δ*H*[‡]_{iso} = 90.0 ± 1.1 kJ mol⁻¹ and

Δ*S*[‡]_{iso} = -21 ± 3 J K⁻¹ mol⁻¹. Under these conditions, the rate law given in eq 4 simplifies to eq 5.

$$k_{\text{iso}} = k_1 + k_3 + (k_2 + k_4)[2]_0 \quad (5)$$

The composition of the associative steps (bimolecular ligand substitutions) considered in Scheme 4 should give negative values of the *apparent* Δ*S*[‡] for the overall process.^{6a} On the contrary, the dissociative mechanism given in Scheme 2 should give very positive values of Δ*S*[‡].^{15,16} Thus, the negative *apparent* value of Δ*S*[‡] obtained is, at least, not in contradiction with the mechanism proposed.

Conclusions

In summary, our results prove that the apparently simple oxidative-addition step framed in Scheme 1 is in fact rather complex: A *cis* isomer is formed first in the addition of RI to Pd(0), which then undergoes isomerization to the more stable *trans* isomer via at least four concurrent bimolecular pathways, two autocatalytic and two solvent-assisted, as shown in Scheme 4.

Experimental Section

The reactions were carried out under N₂. Solvents were purified using standard methods. Pd(PPh₃)₄ and [Pd₂(C₆Cl₂F₃)₂(μ-Cl)₂(tht)₂] were prepared as reported in the literature.^{17,18} Infrared spectra (in cm⁻¹) were recorded on a Perkin-Elmer FT-IR 1720 X spectrometer. Combustion analyses were performed on a Perkin-Elmer 2400 CHN microanalyzer. ¹H, ¹³C{¹H}, ¹⁹F, and ³¹P{¹H} NMR spectra were taken on a Bruker ARX-300 spectrometer equipped with a VT-110 variable-temperature probe; chemical shifts are reported in ppm from Me₄Si (¹H, ¹³C), CCl₃F (¹⁹F), or H₃PO₄ (³¹P) in CDCl₃ at room temperature.

C₆Cl₂F₃I (1). To a solution of [Li(C₆Cl₂F₃)]¹⁸ (21.3 mmol) in diethyl ether (60 mL) at -78 °C was added I₂ (5.65 g, 22.2 mmol), and the mixture was stirred for 2 h while allowing the temperature to increase slowly. The resulting colorless solution was treated with aqueous NaHCO₃, washed with water (2 × 30 mL), and dried over MgSO₄. After evaporation, the solid residue was flash chromatographed (silica/*n*-hexane) and further purified by sublimation in a vacuum (75 °C, 3 mm), yielding white needles of **1** (6.08 g, 87%); mp 42–43 °C. IR (KBr, cm⁻¹): 1591 (m), 1435 (vs), 1069 (vs), 786 (vs), 709 (vs). ¹⁹F NMR (CDCl₃/THF): δ -91.90/-89.47 (d, ⁴J_{FF} = 2.5 Hz, *o*-CF), -110.03/-108.53 (t, ⁴J_{FF} = 2.5 Hz, *p*-CF). ¹³C{¹H} NMR (CDCl₃): δ 156.9 (ddd, ¹J_{FC} = 247.4 Hz, ³J_{FC} = 7.1 Hz, ³J_{FC} = 4.3 Hz, *o*-CF), 155.6 (dt, ¹J_{FC} = 252.5 Hz, ³J_{FC} = 4.6 Hz, *p*-CF), 106.9 (ddd, ²J_{FC} = 27.2 Hz, ²J_{FC} = 21.9 Hz, ⁴J_{FC} = 5.6 Hz, CCl), 66.0 (dt, ²J_{FC} = 31.0 Hz, ⁴J_{FC} = 4.8 Hz, Cl). Anal. Calcd for C₆Cl₂F₃I: C, 22.05. Found: C, 22.03. MS: *m/z* 326 (71) [*M*⁺], 199 (79) [*M*⁺ - I], 164 (72), 149 (68), 127 (100), 79 (94).

***cis*-[Pd(C₆Cl₂F₃)I(PPh₃)₂] (2).** To a suspension of Pd(PPh₃)₄ (268 mg, 0.230 mmol) in THF (11 mL) under N₂ was added **1** (280 mg, 0.860 mmol), and the mixture was stirred at room temperature for 1 h. The solvent was evaporated, and the solid residue was washed with diethyl ether, giving yellow **2** (yield 211 mg, 95%). IR (KBr, cm⁻¹): 1481 (m), 1436 (vs), 1401 (vs), 1195 (s), 1145 (s), 774 (s), 752 (s), 743 (s), 693 (vs), 533 (vs), 521 (vs), 509 (vs), 494 (s). ¹H NMR (CDCl₃): δ 7.5–

(14) These pathways have been proposed for some L-catalyzed *cis*-*trans* isomerizations, see: Cross, R. J. *Adv. Inorg. Chem.* **1989**, *34*, 219–292. The fact that an excess of free PPh₃ does not very noticeably catalyze the isomerization following a pentacoordinate-based mechanism may be due to a higher energy barrier for the pseudorotations.

(15) The dissociation of halide has been proposed for the isomerization of *cis*-[PtRXL₂] complexes in alcoholic solvents, see: Alibrandi, G.; Sclaro, L. M.; Romeo, R. *Inorg. Chem.* **1991**, *30*, 4007–4013 and references therein.

(16) Frey, U.; Helm, L.; Merbach, A. E.; Romeo, R. *J. Am. Chem. Soc.* **1989**, *111*, 8161–8165.

(17) Coulson, D. R. *Inorg. Synth.* **1972**, *13*, 121–123.

(18) Espinet, P.; Martínez-Ilarduya, J. M.; Pérez-Briso, C.; Casado, A. L.; Alonso, M. A. *J. Organomet. Chem.*, in press.

7.3 (m, 3H, CH), 7.2–7.1 (m, 2H, CH). ¹⁹F NMR (CDCl₃/THF/PhCl): δ -90.63/-85.87/-85.90 (dd, ⁴J_{FP} = 12.0 Hz, ⁴J_{FP'} = 6.0 Hz, *o*-CF), -120.83/-118.32/-116.63 (dd, ⁶J_{FP} = 1.1 Hz, ⁶J_{FP'} = 2.5 Hz, *p*-CF). ³¹P{¹H} NMR (CDCl₃/THF/PhCl): δ 29.6/33.3/33.4 (ddt, ²J_{PP} = 26.9 Hz, ⁴J_{FP} = 5.9 Hz, ⁶J_{FP} = 2.5 Hz), 16.7/21.0/21.0 (ddt, ²J_{PP} = 26.9 Hz, ⁴J_{FP} = 11.9 Hz, ⁶J_{FP} = 1.2 Hz). Anal. Calcd for C₄₂H₃₀Cl₂F₃IPd: C, 52.67; H, 3.16. Found: C, 52.94; H, 3.45.

trans-[Pd(C₆Cl₂F₃)Cl(PPh₃)₂] (4). To a stirred suspension of [Pd₂(μ-Cl)₂(C₆Cl₂F₃)₂(tht)₂] (250 mg, 0.291 mmol) in acetone (10 mL) was added PPh₃ (305 mg, 1.16 mmol). After a fast solubilization, white **4** immediately precipitated. The mixture was stirred for 1 h, and then the acetone evaporated. The solid residue was recrystallized from CH₂Cl₂/*n*-hexane at -28 °C, and the resulting colorless crystals were washed with ethanol and air-dried (yield 484 mg, 96%). IR (KBr, cm⁻¹): 1587 (m), 1481 (s), 1435 (vs), 1402 (vs), 1096 (vs), 1048 (s), 776 (s), 743 (s), 693 (vs), 522 (vs), 512 (vs), 496 (s), 428 (s), 314 (s). ¹H NMR (CDCl₃): δ 7.7–7.6 (m, 2H, CH), 7.45–7.30 (m, 3H, CH). ¹⁹F NMR (CDCl₃): δ -91.50 (t, ⁴J_{FP} = 7.2 Hz, *o*-CF), -121.19 (t, ⁶J_{FP} = 2.6 Hz, *p*-CF). ³¹P{¹H} NMR (CDCl₃): δ 24.7 (td, ⁴J_{FP} = 7.2 Hz, ⁶J_{FP} = 2.6 Hz). Anal. Calcd for C₄₂H₃₀Cl₃F₃P₂Pd: C, 58.23; H, 3.49. Found: C, 58.01; H, 3.57.

trans-[Pd(C₆Cl₂F₃)I(PPh₃)₂] (3). To a colorless solution of **4** (400 mg, 0.462 mmol) in acetone/CH₂Cl₂ (5/5 mL) was added an excess of NaI (200 mg, 1.33 mmol). The resulting yellow mixture was stirred at room temperature for 1 h and evaporated to dryness. The residue was extracted in CH₂Cl₂ and evaporated to dryness, yielding yellow **3**, which was washed with diethyl ether and vacuum-dried (yield 376 mg, 85%). IR (KBr, cm⁻¹): 1589 (w), 1482 (m), 1435 (vs), 1404 (vs), 1097 (s), 1048 (s), 773 (s), 742 (s), 692 (vs), 522 (vs), 512 (vs), 495 (s). ¹H NMR (CDCl₃): δ 7.7–7.6 (m, 2H, CH), 7.4–7.3 (m, 3H, CH). ¹⁹F NMR (CDCl₃/THF/PhCl): δ -92.48/-88.17/-87.91 (t, ⁴J_{FP} = 6.6 Hz, *o*-CF), -120.80/-117.65/-116.34 (t, ⁶J_{FP} = 2.5 Hz, *p*-CF). ³¹P{¹H} NMR (CDCl₃/THF): δ 22.6/26.9/26.8 (td, ⁴J_{FP} = 7.2 Hz, ⁶J_{FP} = 2.5 Hz). Anal. Calcd for C₄₂H₃₀Cl₂F₃IP₂Pd: C, 52.67; H, 3.16. Found: C, 52.99; H, 3.59.

Kinetic experiments. NMR tubes (5 mm) were charged with appropriate amounts of **2**, which was dissolved under N₂ at room temperature (293 K) in THF to a fixed volume of 600 ± 5 μL (obtaining the concentrations shown in Table 1). An acetone-*d*₆ capillary was used for deuterium lock. The tube was placed in a thermostated probe (±0.2 K, the temperature was measured by ethylene glycol or methanol standard methods). Concentration vs time data were then acquired from ¹⁹F NMR signal areas of **2** and **3** and fitted to the equation ln([**2**]) vs *t* to obtain first-order constants *k*_{iso} from least-squares slopes (standard errors are also given). A strictly oxygen-free N₂ atmosphere is required in the kinetic experiments. When

traces of oxygen are present, easy phosphine oxidation occurs and the defect of phosphine accelerates the isomerization very noticeably, giving ln([**2**]) vs *t* plots with marked curvature. OPPh₃ was detected after an experimental run in the presence of some air using ³¹P{¹H} NMR: δ 28.4 ppm in THF at room temperature. This phosphine oxidation interference was more evident in THF than in chlorobenzene.

Acknowledgment. Financial support by the Dirección General de Investigación Científica y Técnica (Project No. PB96-0363) and the Junta de Castilla y León (Project No. VA40/96) and a fellowship to A.L.C. from the Ministerio de Educación y Ciencia are very gratefully acknowledged.

Appendix: Derivation of Kinetic Eq 4. The steady-state concentrations of intermediates **A** and **B**, and the isomerization rate, are given in eqs 6–10.

$$[\mathbf{A}] = \frac{k_3[\mathbf{2}] + k_{-5}[\mathbf{B}]}{k_{-3}[\text{PPh}_3] + k_5[\mathbf{2}]_0} \quad (6)$$

$$[\mathbf{B}] = \frac{k_4[\mathbf{2}][\mathbf{2}]_0 + k_5[\mathbf{A}][\mathbf{2}]_0}{k_{-4}[\text{PPh}_3] + k_{-5} + k_6} \quad (7)$$

$$[\mathbf{B}] = \frac{k_3k_5 + k_4(k_5[\mathbf{2}]_0 + k_{-3}[\text{PPh}_3])}{k_{-3}k_{-5}[\text{PPh}_3] + (k_{-4}[\text{PPh}_3] + k_6)(k_{-3}[\text{PPh}_3] + k_5[\mathbf{2}]_0)} [\mathbf{2}][\mathbf{2}]_0 \quad (8)$$

$$r_{\text{iso}} = \{k_1 + k_2[\mathbf{2}]_0\}[\mathbf{2}] + k_6[\mathbf{B}] \quad (9)$$

$$r_{\text{iso}} = \{k_1 + k_2[\mathbf{2}]_0\}[\mathbf{2}] + \frac{k_3k_5k_6 + k_4k_6(k_5[\mathbf{2}]_0 + k_{-3}[\text{PPh}_3])}{k_{-3}k_{-5}[\text{PPh}_3] + (k_{-4}[\text{PPh}_3] + k_6)(k_{-3}[\text{PPh}_3] + k_5[\mathbf{2}]_0)} [\mathbf{2}] [\mathbf{2}]_0 \quad (10)$$

If we consider that *k*₋₃[PPh₃] is low, eq 10 can be simplified to eq 4.

$$k_{\text{iso}} = k_{\text{iso}}[\mathbf{2}] = \left\{ k_1 + k_2[\mathbf{2}]_0 + \frac{k_3k_6 + k_4k_6[\mathbf{2}]_0}{k_{-4}[\text{PPh}_3] + k_6} \right\} [\mathbf{2}] \quad (4)$$

OM9709502